

Fourier-based analysis of moiré fringe patterns of superposed gratings in alignment of nanolithography

Shaolin Zhou,^{1,2*} Yongqi Fu,¹ Xiaoping Tang,¹ Song Hu,¹ Wangfu Chen,^{1,2} and Yong Yang,^{1,2}

¹ Institute of optics & electronics, Chinese Academy of sciences, Chengdu 610209, China;

² Graduate School of Chinese Academy of Sciences, Beijing 100039, China

* Corresponding author: xiangyayong@163.com

Abstract: Considering the necessity of alignment in practical applications of photolithography, distribution of complex amplitude of moiré fringe patterns that are produced in superposition of two gratings is analyzed in the viewpoint of Fourier Optics and the relationship between fringes and properties of these two gratings is concluded by means of an analysis model. The rule of one-dimensional gratings (1D-gratings) is extended to other form of the gratings which have quasi-periodic repetitive structures. Especially, moiré fringes generated by the two superposed 1D-gratings (used in alignment of lithography) can be expressed by an arithmetical operation of two vectors which include enough information about these 1D-gratings. Numerical analyses regarding the moiré model and its application in the alignment process of lithography are carried out. Our computational analyses results show that the moiré fringes of the two extended gratings can be refined as a transformed fringe pattern of two standard 1D-gratings. Finally, the results also make it out that the fringes which have magnified periods versus that of two 1D-gratings are highly sensitive to relative shift of two gratings thus might be applicable in alignment of lithography or correlated fields.

©2008 Optical Society of America

OCIS codes: (070.0070) Fourier optics; (050.2770) Gratings; (220.1140) Alignment; (120.4120) Moiré techniques

References and links

1. L. Raleigh, "On the manufacture and theory of diffraction gratings," *Philos. Mag.* **4**, 81-93 (1874).
2. J. Gaid, *The Interference Systems of Crossed Diffraction Gratings* (Oxford University Press, London, 1956).
3. J. Gaid, *Diffraction Gratings as Measuring Scales*, (Oxford University Press, London, 1960).
4. I. G. O.Kafri, *The Physics of Moire Metrology*, (Wiley, New York, 1989).
5. G. Oster, M. Wasserman, and C. Zwerling, "Theoretical Interpretation of Moiré Patterns," *J. Opt. Soc. Am. A* **54**, 169-175 (1964).
6. Y. Nishijima and G. Oster, "Moiré Patterns: Their Application to Refractive Index and Refractive Index Gradient Measurements," *J. Opt. Soc. Am. A* **54**, 1-5 (1964).
7. O. Bryngdahl, "Moiré: Formation and interpretation," *J. Opt. Soc. Am. A* **64**, 1287-1294 (1974).
8. O. Bryngdahl, "Moiré and higher grating harmonics," *J. Opt. Soc. Am. A* **65**, 685-694 (1975).
9. I. Amidror and R. D. Hersch, "Fourier-based analysis of phase shifts in the superposition of periodic layers and their moire effects," *J. Opt. Soc. Am. A* **13**, 974-987 (1996).
10. I. Amidror and R. D. Hersch, "Fourier-based analysis and synthesis of moirés in the superposition of geometrically transformed periodic structures," *J. Opt. Soc. Am. A* **15**, 1100-1113 (1998).
11. M. C. King and D. H. Berry, "Photolithographic mask alignment using moire techniques," *J. Vac. Sci. Technol. B* **11**, 2455-2458 (1972).
12. K. Hara, Y. Uchida, T. Nomura, S. Kimura, D. Sugimoto, A. Yoshida, H. Miyake, T. Iida, and S. Hattori, "An alignment technique using diffracted moire signals," *J. Vac. Sci. Technol. B* **7**, 1977-1979 (1989).
13. A. Moel, E. E. Moon, R. D. Frankel, and H. I. Smith, "Novel on-axis interferometric alignment method with sub-10 nm precision," *J. Vac. Sci. Technol. B* **11**, 2191-2194 (1993).

14. J. H. Lee, C. H. Kim, Y.-S. Kim, K. M. Ho, K. Constant, W. Leung, and C. H. Oh, "Diffracted moiré fringes as analysis and alignment tools for multilayer fabrication in soft lithography," *Appl. Phys. Lett.* **86**, 204101-204101 -- 204101-204103 (2005), [DOI: 10.1063/1.1927268]
15. N. H. Li, W. Wu, and S. Y. Chou, "Sub-20-nm alignment in nanoimprint lithography using Moiré fringe," *Nano Lett.* **6**, 2626-2629 (2006).
16. M. Muhlberger, I. Bergmair, W. Schwinger, M. Gmainer, R. Schoftner, T. Glinsner, C. Hasenfuss, K. Hingerl, M. Vogler, H. Schmidt, and E. B. Kley, "A Moiré method for high accuracy alignment in nanoimprint lithography," *Microelectron. Eng.* **84**, 925-927 (2007).
17. L. Q. T, *Physical Optics*, (China Machine Press, Beijing, 1986).

1. Introduction

Moiré fringe is a phenomenon that occurs in the superposition of two repetitive structures such as gratings. Lord Raleigh pointed out that two overlapped 1D-gratings can produce a set of low-frequency fringes which is relevant to quality of the gratings in 1874.[1] Therefore, the moiré fringes was firstly employed for the purpose of evaluating the quality of gratings[2] and metrology.[3, 4] Thereafter, systematic geometrical and algebraic analysis about the moiré fringes in the superposed repetitive structures was performed to explain this phenomenon.[5] Then moiré fringe phenomenon was applied to the measurement of both refractive index and refractive index gradient.[6] Fourier-based approach that can systematically interpret the properties of moiré fringes in overlapped repetitive structures was eventually shown to be more effective due to the complexity of the previous classical algebraic and geometric analysis.[7-10]

More recently, the necessity of high resolution in photolithography promotes the application of moiré fringes in the alignment process of photolithography such as alignment in nanoimprint.[11-16] From circular moiré fringes used for manual alignment of early times to the 1D-distributed moiré fringes used for high resolution automatic alignment, the moiré-based technique has been adopted for alignment of photolithography. Therefore, considering more application of the moiré-based alignment technique in this or correlated fields, deep research about moiré fringes of certain gratings used in alignment of lithography is performed in this paper. The relationship between the moiré fringes properties and the geometrical layout of gratings is briefly discussed, and analysis models of the moiré fringes which occur in the two superposed gratings is also built in the view of Fourier Optics. Specifically, the rule of moiré fringes produced by two 1D-gratings (used in alignment of lithography) is expressed by an arithmetic operation of two vectors. Some results would be a theoretical guideline for the alignment of photolithography and other design of moiré-based metrological technique. Under a certain circumstance, the results are applicable to the superposition of several gratings (more than two).

2. Theoretical models

2.1 Transmittance model of gratings and Fourier decomposition

In practical applications, gratings appear to be circular, elliptical or some other geometrical shape besides the common 1D-grating. Additionally, these gratings may have different profiles corresponding to different transmittance coefficients such as square wave, sinusoidal, and saw-tooth etc. Our analyses start from the common 1D-grating and the transmittance model of all gratings is deduced. The transmittance model can be defined as a periodic function because of periodicity of grooves of gratings. Therefore, the transmittance coefficient of 1D-gratings with rectangular profile can be expressed as

$$G(x') = \sum_{n=-\infty}^{+\infty} \text{rect}\left(\frac{x'-np}{d}\right) \quad (1)$$

Where, p is the period of grating and d is the width of grooves of grating. The transmittance coefficient can be expressed as an accumulation of a rectangle function $\text{rect}(x)$. The gratings with other profiles can be defined in the same way. Hereinafter, we use the gratings with

rectangular profile as an example to continue our analysis and gratings that can be expressed as the form of Eq. (1) are called standard 1D-gratings.

For simplicity we begin with standard 1D-gratings, whereas gratings with other geometrical layout is considered as extended coordinate-transformed structures which can be obtained by applying a geometric transformation such as bend or rotation to a standard 1D-grating. Therefore, by replacing x' with a certain function $T(x, y)$ in Eq. (1), the 1D-gratings can be transformed into other curvilinear gratings. Here, $T(x, y) = C$ denotes the layout of certain quasi-periodic structures as in Fig. 1. For each determined variable constant C , this expression denotes a determined curve (like the particular nT grooves of 1D-gratings) among the transformed repetitive structures. As a result, a model of transmittance coefficient for the quasi-periodic repetitive structures can be obtained by the same way used in Eq. (1).

$$G_T(x, y) = G[T(x, y)] = \sum_{n=-\infty}^{+\infty} \text{rect}\left(\frac{T(x, y) - np}{d}\right) \quad (2)$$

Where, the accumulation of rectangle function means that the profile of these transformed structures remains rectangular and $T(x, y)$ denotes the shape of them.

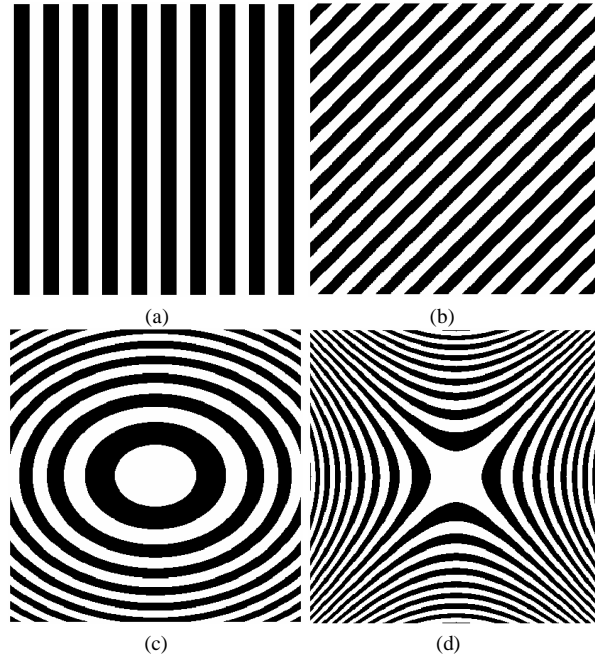


Fig. 1. Standard 1D-grating and the transformed structures: (a) standard 1D-grating with standardized period, (b) rotated 1D-grating with $T(x, y) = y - x$, (c) ellipse-shaped structures with $T(x, y) = y^2/9 + x^2/16$, (d) parabola-shaped structures with $T(x, y) = y^2 - x^2$.

According to Fourier Optics, the distribution of complex amplitude of diffractive wave $E(x, y)$ in the plane close to the back of gratings accords with the transmittance coefficient of gratings, [17] namely $E(x, y) = G_T(x, y)$. Furthermore, the diffractive wave can also be regarded as an accumulation of different harmonics with discrete frequencies because of the periodicity of the gratings. When the planar wave with unit amplitude travels through the 1D-grating, the complex amplitude of the diffractive wave can therefore be decomposed as

$$E(x') = \int_{-\infty}^{+\infty} E(f) \exp(i2\pi f x') df = \sum_{n=-\infty}^{+\infty} a_n \exp(i2\pi n f_0 x') \quad (3)$$

Where, $E(f) = \sum_{n=-\infty}^{+\infty} a_n \delta(f - nf_0)$ is the spectrum of the diffractive wave traveled through the 1D-grating, $a_n = df_0 \sin c(ndf_0)$ is Fourier coefficient of rectangular function in Eq. (1) and $f_0=1/p$. In the same way, the Fourier model of distribution of complex amplitude for those extended repetitive structures can be expressed as

$$E_T(x, y) = \sum_{n=-\infty}^{+\infty} a_n \exp[i2\pi n f_0 T(x, y)] \quad (4)$$

2.2 Extraction model of moiré fringes distributions

Moiré fringes appear in the overlay of the repetitive structures and vary in terms of the geometrical layout of the superposed structures. The rule of how moiré fringes be modulated by such quasi-period repetitive structures is briefly discussed below.

2.2.1 Moiré fringes distributions

Likewise we start with two standard 1D-gratings, the frequencies of which are assumed to be f_1 and f_2 . Then two gratings with the extended layout can be obtained by applying certain two transformations $T_1(x, y)$ and $T_2(x, y)$ to these two standard 1D-gratings respectively. As the discussion above, the complex amplitude of the diffractive wave behind two extended structures can be respectively expressed as

$$E_1(x, y) = G_1(x, y) = \sum_{n=-\infty}^{+\infty} a_n \exp[i2\pi n f_1 T_1(x, y)]$$

$$E_2(x, y) = G_2(x, y) = \sum_{m=-\infty}^{+\infty} b_m \exp[i2\pi m f_2 T_2(x, y)]$$

When the planar wave with unit amplitude travels through these two superposed gratings, the amplitude of the diffractive wave behind the second grating can be written as

$$E(x, y) = E_1(x, y)E_2(x, y)$$

$$= \sum_{m=-\infty}^{+\infty} \sum_{n=-\infty}^{+\infty} a_n b_m \exp\{i2\pi[mf_2 T_2(x, y) + nf_1 T_1(x, y)]\} \quad (5)$$

We extract the partial sum in Eq. (5) and translate it into the same form as Eq. (4), namely

$$E(x, y) = \sum_{n=-\infty}^{+\infty} a_{nk_1} b_{nk_2} \exp\{i2\pi n f [k_1 \cdot f_1 / f \cdot T_1(x, y) + k_2 \cdot f_2 / f \cdot T_2(x, y)]\} \quad (6)$$

Where k_1, k_2 are the integers except 0, and f is the standardized frequency. Thus twofold sum of Eq. (5) is decomposed into many partial sums. Compared with Eq. (4), Eq. (6) can be regarded as the form obtained by applying a compound transformation of $T(x, y)$ to $E(x')$, which can be considered as the complex amplitude distribution of the diffractive wave behind certain 1D-gratings (the profile of which may not be rectangular any longer) with standard frequency f . Here, we have

$$E(x') = \sum_{n=-\infty}^{+\infty} a_{nk_1} b_{nk_2} \exp(i2\pi n f x') \quad (7)$$

$$T(x, y) = k_1 \cdot f_1 / f \cdot T_1(x, y) + k_2 \cdot f_2 / f \cdot T_2(x, y) \quad (8)$$

Obviously for every (k_1, k_2) , partial sum series in Eq. (7) will converge to a periodic-distributed pattern which is similar to the layout of standard 1D-gratings, and this pattern would become another patterns denoted by Eq. (6) while transformed by $T(x, y)$ in Eq. (8). We

call the pattern denoted by Eq. (6) (k_1, k_2) moiré fringes and the pattern denoted by Eq. (7) standard 1D moiré fringes. This process can be concluded as that moiré fringes generated by superposition of two geometrically transformed 1D-gratings are equivalent to the patterns obtained by application of a compound transformation to a certain 1D-distributed moiré fringes. We call it “*conclusion 1*” hereinafter. The relationship between the 1D-distributed moiré fringes and these two 1D-gratings can be described by Eq. (7), whereas the relationship between the compound transformation and two transformations of the original 1D-gratings can be expressed by Eq. (8).

2.2.2 Analysis of 1D-distributed moiré fringes

The rule of periodic 1D-distributed moiré fringes generated by superposition of two 1D-gratings is discussed in this part. We consider these two 1D-gratings as rotated standard 1D-gratings and these two rotational transformations are assumed to be

$$T_1(x, y) = x \sin \theta_1 - y \cos \theta_1 \quad (9)$$

$$T_2(x, y) = x \sin \theta_2 - y \cos \theta_2 \quad (10)$$

Where, θ_1 is slope of the rotated 1D-grating with frequency of f_1 (seen in Fig. 2(b)) and θ_2 is the slope of the other 1D-grating with frequency of f_2 . And the complex amplitude of (k_1, k_2) moiré fringes behind these two superposed gratings can be obtained according to Eq. (6) and standardized according to Eq. (4) as

$$E(x, y) = \sum_{n=-\infty}^{+\infty} a_{nk_1} b_{nk_2} \exp[i2\pi n f_e (x \sin \theta_e - y \cos \theta_e)] \quad (11)$$

Here we let $T_e(x, y) = x \sin \theta_e - y \cos \theta_e$, where θ_e, f_e are slope and frequency of moiré fringes respectively.

We can draw a conclusion that when two standard 1D-gratings with frequencies of f_1 and f_2 are individually rotated by $T_1(x, y)$ and $T_2(x, y)$ in Eq. (9) and Eq. (10), the (k_1, k_2) moiré fringes generated by two rotated gratings can be regarded as a set of standard 1D-fringes with frequency of f_e rotated by $T_e(x, y)$ in Eq. (11). Furthermore, the rotated fringes can be expressed by a vector which is the sum of two vectors on be half of two original 1D-gratings. We called it “*conclusion 2*” hereinafter.

Here we resorted to the vector $\vec{F}_1 = k_1 f_1 \exp(i \theta_1)$ to denote the 1D-grating with frequency f_1 and slope θ_1 , $\vec{F}_2 = k_2 f_2 \exp(i \theta_2)$ to denote the other 1D-grating with frequency f_2 and slope θ_2 respectively. As a result, the vector $\vec{F}_e = f_e \exp(i \theta_e)$ on be half of their moiré fringes can be obtained by sum of \vec{F}_1 and \vec{F}_2 , namely $\vec{F}_e = \vec{F}_1 + \vec{F}_2$. Thus

$$\begin{aligned} f_e \cos \theta_e &= k_1 f_1 \cos \theta_1 + k_2 f_2 \cos \theta_2 \\ f_e &= \left| \vec{F}_e \right| = \sqrt{(f_1 k_1)^2 + (f_2 k_2)^2 + 2 f_1 f_2 k_1 k_2 \cos(\theta_1 - \theta_2)} \end{aligned} \quad (12)$$

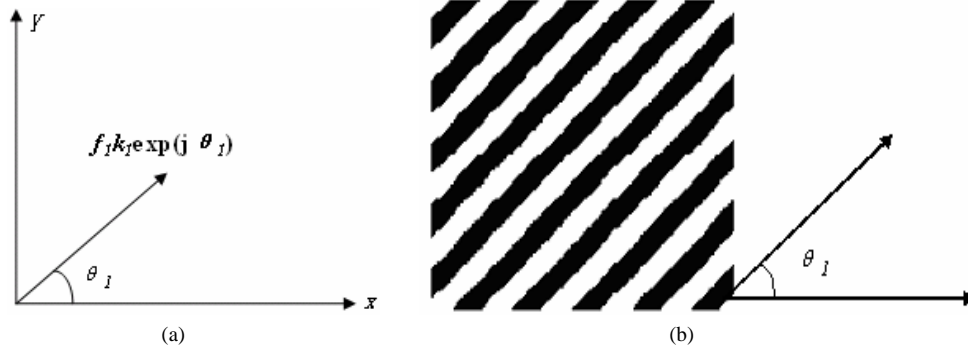


Fig. 2. (a). The descriptive vector and (b) its corresponding rotated 1D-grating

Obviously the slope of grooves of the 1D-grating is the same as that of corresponding vector (seen in Fig. 2). And these descriptive vectors include enough information about grooves of 1D-gratings or that of corresponding fringes. Furthermore, the conclusion indicates that the two superposed 1D-gratings generate 1D-distributed moiré fringes. The frequency and slope of (k_1, k_2) moiré fringes are correlated with that of two 1D-gratings. Obviously the conclusion can be extended to a superposition of more 1D-gratings and the vector of corresponding fringes can be expressed as a sum of more vectors which denote every 1D-grating.

Actually, whether or not the moiré fringes are visible to our human eye strongly depends on the fact that if the frequency of the moiré fringes locates in the resolvable spectrum of visual systems. Usually, the (1,-1) moiré fringes frequency of which appears to the lowest can be resolved by human eye.

2.2.3 Analysis of special moiré fringes distributions

The (1,-1) moiré fringes resolvable by human eye achieve broad applications and we discuss them in this part. Generally, moiré fringes generated by two superposed gratings that are transformed from two standard 1D-gratings with *different frequencies* by *different transformations* are in accordance with the rule of *conclusion 1*. Whereas, according to Eq. (6) no resolvable fringes are generated by two gratings transformed from two 1D-gratings with the *same frequency* by *the same transformation* because the (1,-1) moiré fringes disappeared. Especially, Eq. (12) indicates that the two superposed 1D-gratings with the same frequency and the same slope generated no resolvable fringes because the (1,-1) moiré fringes disappeared too. The moiré fringes of the two superposed 1D-gratings with different frequencies and different slopes are in accordance with the rule of *conclusion 2*. Therefore, we had four cases here: *different frequencies vs. different transformations*, *the same frequency vs. the same transformation*, *the same frequency vs. different transformations*, and *different frequencies vs. the same transformation*. The other two cases are discussed below in detail.

A. *The same frequency vs. different transformations*. When two superposed gratings are transformed from the same standard 1D-grating with frequency of f by different transformations T_1 and T_2 , the amplitude distribution of the (1,-1) moiré fringes can be deduced from Eq. (6) as

$$E(x, y) = \sum_{n=-\infty}^{+\infty} a_n b_{-n} \exp\{i2\pi n f [T_1(x, y) - T_2(x, y)]\} \quad (13)$$

Obviously, the fringes denoted by Eq. (13) can be considered as a set of standard 1D-distributed moiré fringes transformed by the difference of two original transformations, Namely, $T_1(x, y) - T_2(x, y)$. Especially, if two superposed gratings are rotated 1D-gratings, their descriptive vectors is $\vec{F}_1 = f_1 \exp(i\theta_1)$ and $\vec{F}_2 = f_2 \exp(i\theta_2)$. Correspondingly, the vector

\vec{F}_e which on behalf of the 1D-distributed moiré pattern can be expressed as the *difference* of vectors \vec{F}_1 and \vec{F}_2 according to the *conclusion 2*, namely $\vec{F}_e = \vec{F}_1 - \vec{F}_2$.

B. The same transformation vs. different frequencies. According to Eq. (6), the complex amplitude distribution of (1,-1) moiré fringes produced by two superposed gratings that are transformed from two standard 1D-gratings with different frequencies f_1 and f_2 by the same transformation T can be expressed as

$$E(x, y) = \sum_{n=-\infty}^{+\infty} a_n b_{-n} \exp[i2\pi n(f_1 - f_2)T(x, y)] \quad (14)$$

Here, we assume that f_1 is slightly bigger than f_2 , namely $f_1 > f_2$. Obviously the pattern denoted by Eq. (14) can be regarded as a set of standard 1D-distributed moiré fringes with frequency of $f_1 - f_2$ transformed by the same function T . Now the period of the low-frequency fringes is magnified with respect to that of two original gratings, namely $p = 1/|f_1 - f_2| = p_1 p_2 / (p_2 - p_1)$.

We continue to assume that two transformations are $T_1 = x + \Delta x$ and $T_2 = x$, i.e. the 1D-gratings with frequency f_1 move left by Δx with respect to the other 1D-grating. The moiré fringes distribution before and after movement can be respectively expressed as

$$E_p(x, y) = \sum_{n=-\infty}^{+\infty} a_n b_{-n} \exp[i2\pi n[(f_1 - f_2)x]] \quad (15)$$

$$E_a(x, y) = \sum_{n=-\infty}^{+\infty} a_n b_{-n} \exp\{i2\pi n[(f_1 - f_2)x + f_1 \cdot \Delta x]\} \quad (16)$$

In comparison to the two equations above, we conclude that relative move of these two gratings will change the spatial phase of the fringes distribution. A left shift of Δx of the grating with frequency f_1 leads to a left shift of $\Delta x f_1 / (f_1 - f_2) = \Delta x p_2 / (p_2 - p_1)$ of the fringes. Vice versa, a left shift Δx of the grating with frequency f_2 results in a left shift of the fringes by $\Delta x p_1 / (p_2 - p_1)$. Therefore, the phenomenon that tiny displacement of a grating leads to large displacement of corresponding moiré fringes can be applied in some fields such as the alignment of nanolithography.

3. Results analyses and discussions

Two conclusions are drawn above to describe the rule of how moiré fringes distribution change with the layout of the quasi-period structures, especially for how 1D-distributed moiré fringes distribution change with the layout of two 1D-gratings. Here simulation based analyses and discussions about the (1,-1) moiré fringes are carried out and stated below.

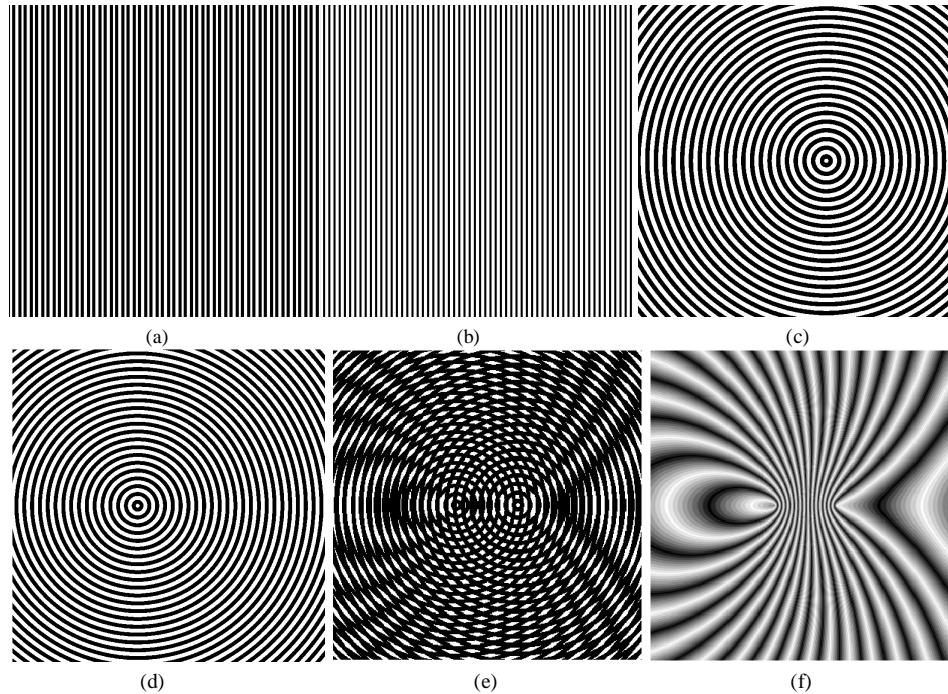


Fig. 3. (a). Standard 1D-grating with standardized frequency of 1. (b): standard 1D-grating with frequency of 0.9. (c) and (d) show two circular gratings that are obtained by application of the transformation: $T_1(x, y) = [(x+4)^2 + y^2]^{1/2}$ and $T_2(x, y) = [(x-4)^2 + y^2]^{1/2}$ to 1D-gratings in (a) and (b). (e): moiré pattern generated from superposition of these two circular gratings with centers offset by 8 units. (f): the (1,-1) moiré fringe extracted according to *conclusion 1*.

Two sets of gratings with slightly different frequencies and corresponding moiré fringes are illustrated in Fig. 3. Figure 3(e) shows the observed moiré fringes of the two circular gratings with centers off-set by 8 periods (seen in Fig. 3(c) and Fig. 3(d)). The (1,-1) moiré fringes that are extracted by applying the compound transformation $T_1(x, y) - 0.9T_2(x, y)$ to the standard 1D-distributed moiré fringes denoted by Eq. (7) are shown in Fig. 3(f). These two results indicate that the (1,-1) moiré fringes extracted according to the rule of *conclusion 1* are the same as the fringes directly observed from superposition of two corresponding gratings.

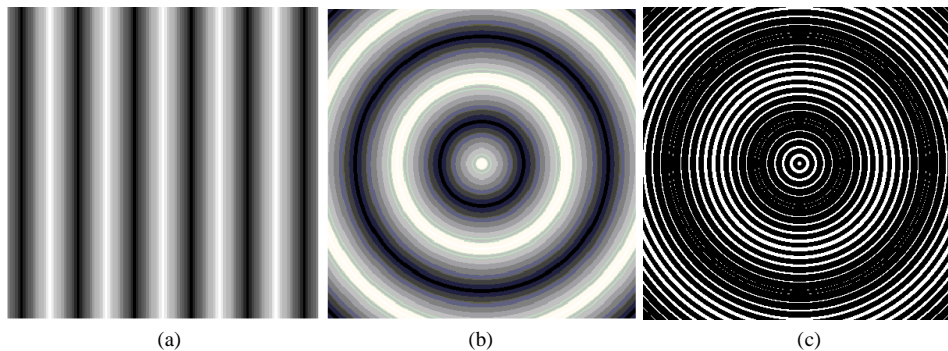


Fig. 4. (a). 1D-distributed moiré of two superposed standard 1D-gratings in Fig. 1(b), the (1,-1) moiré fringe extracted from two circular gratings with centers superposed according to *conclusion 1*. (c): Circular moiré fringe directly observed from two circular gratings with centers superposed.

Figure 4 show moiré fringes generated by two superposed gratings that were transformed from two standard 1D-gratings (seen in Fig. 3) with *slightly different frequencies* by the *same*

transformation. It is apparent that moiré fringes obtained in the two different approaches are the same, and the period of the fringes is magnified with respect to that of two original 1D-gratings. Take the 1D-grating with the period $p_1=1/0.9$ in Fig. 3(b) for example, the period of its moiré fringes in Fig. 4(a) is magnified by $p_1/|p_1-p_2|\approx 10$ times. As the discussions in section 2.2.3 B, this result can be interpreted that the frequency of (1,-1) moiré fringes generated by the two superposed gratings with *slightly different frequencies* equals to the difference of two original frequencies. Likewise, the transverse displacement of two gratings led to a magnified displacement of corresponding moiré fringes.

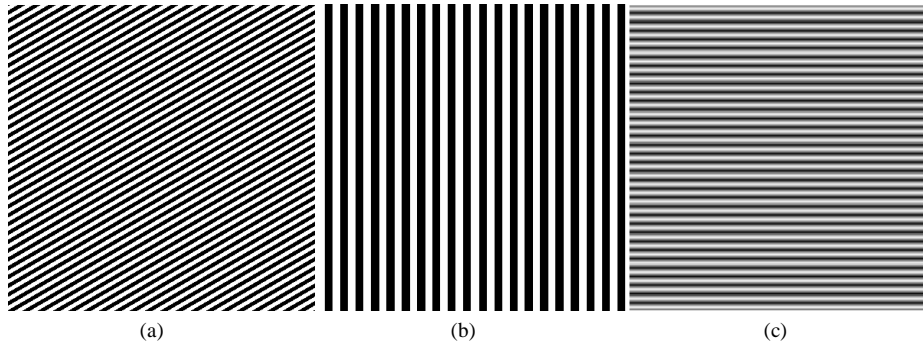


Fig. 5. (a). A 1D-grating denoted by $\vec{F}_1 = 2 \cdot \exp(i\pi/6)$. (b). A 1D-grating denoted by $\vec{F}_2 = \exp(i\pi/2)$. (c): moiré fringes generated by 1D-gratings in (a) and (b).

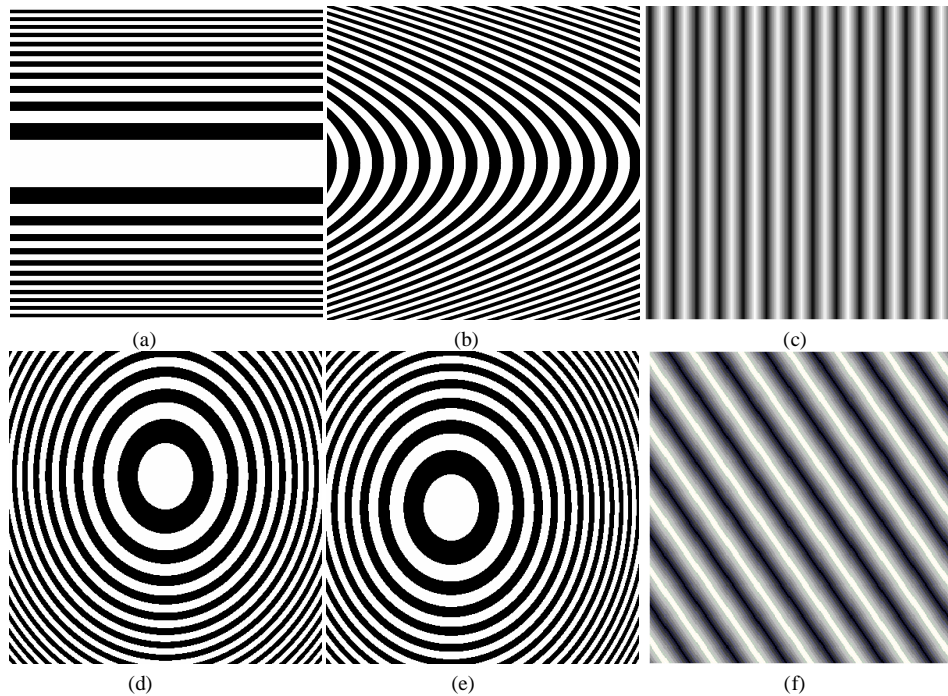


Fig. 6. (a) and (b) are two structures transformed from the same standard 1D-grating with frequency of 1 by $T_1(x, y) = x/3 + y^2/36$ and $T_2(x, y) = y^2/36$. (c) is the moiré fringes of two superposed structures in (a) and (b). (d) and (e) are two elliptic structures transformed from the same standard 1D-grating by $T_1(x, y) = x^2/25 + (y-4)^2/36$ and $T_2(x, y) = (x+4)^2/25 + y^2/36$. (f) is the extracted moiré fringes of two superposed structures in both (d) and (e).

Two 1D-gratings and their 1D-distributed moiré fringes are shown in Fig. 5. Figure 5(a) shows one grating with the frequency of $f_1=2$ and slope of $\theta_1=30^\circ$. Figure 5(b) shows the other standard 1D-gratings with frequency $f_2=1$ and slope $\theta_2=90^\circ$. According to the vector's arithmetic operation rule drawn in *conclusion 2*, (1, -1) moiré fringes of these two 1D-gratings can be expressed by the vector $\vec{F}_1 - \vec{F}_2 = 3^{1/2}$ which means that the frequency and slope of their moiré fringes is $f_e=3^{1/2}$ and $\theta_e=0^\circ$. The extracted (1,-1) moiré fringes shown in Fig. 5(c) prove in accordance with this result.

Figure 6 shows two sets of 1D moiré fringes extracted in the superposition of two couples of quasi-periodic structures according to the *conclusion 1*. And each couple of these quasi-periodic structures is transformed from the same standard 1D-grating by different transformations T_1 and T_2 . Significantly, each set of fringes can be considered as that a set of standard 1D-distributed moiré fringes are transformed by the difference of two corresponding transformations T_1 and T_2 . This result also indicates that the superposition of the curvilinear structures may also generate 1D-distributed moiré fringes and the layout of gratings can be synthesized according to the distribution of the corresponding fringes.

4. Applicability in alignment of nanolithography

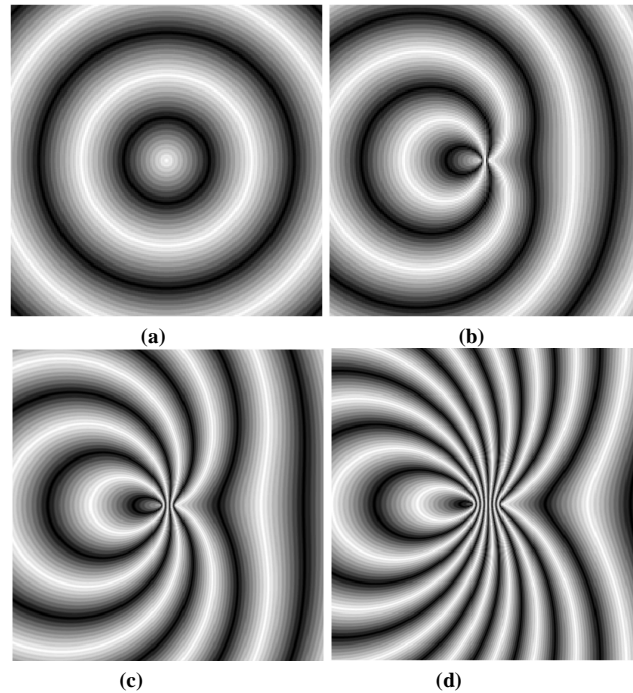


Fig. 7. the circular moiré pattern of two superposed circular gratings marks with centers offset by (a) 0 units; (b) 1 unit; (c) 2 units; (d) 4 units.

According to the discussions in Section 2.2.3 B and computational results in Section 3, superposition of two gratings with the same layout and slightly different periods lead to a set of moiré fringes with the same layout and magnified period with respect to that of original gratings. Furthermore, the phenomenon that a relative transverse displacement of these two superposed gratings leads to a magnified transverse displacement of the moiré fringes can be applied to fields where high sensitivity is required such as the alignment of nanolithography.

In application of alignment of lithography, the superposition of the two grating marks on both the wafer and mask leads to a magnified fringes, the distribution of which can indicate the alignment of the two marks. Figure 7 shows several moirés fringes generated by the

superposition of two circular gratings marks with standardized frequencies $f_1=1$ and $f_2=0.9$ in the alignment of photolithography. Figure 7(a) shows moiré fringes of two aligned marks and fringes in Figs. 7(b)-7(d) correspond to two superposed marks that are misaligned by 1, 2, and 4 grating periods, respectively. We can also make it out from Fig. 7 that the number of misaligned grating periods is half the number of curves that pass through the common point in the pattern.

Apart from circular gratings, 1D-gratings can also be used in alignment of lithography. Figure 8 show two different grating marks and their moiré fringes corresponding to different misaligned grating periods. Figure 8(a) is the mark placed on the wafer and Fig. 8(b) is the mark placed on the mask. According to the discussion in Section 2.2.3 B, we can deduce that a relative transverse movement of Δx leads to a magnified reverse shift ΔL of the two sets of moiré fringes on the pattern, that is

$$\Delta L = \Delta x p_1 / (p_2 - p_1) + \Delta x p_2 / (p_2 - p_1) = \Delta x (p_1 + p_2) / p_2 - p_1 \quad (17)$$

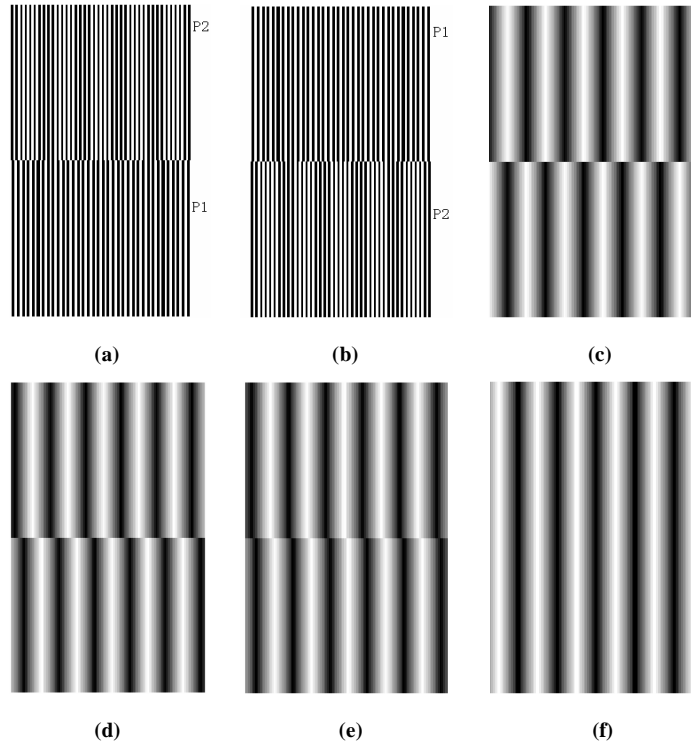


Fig. 8. (a). The grating mark on the wafer. (b) The grating mark on the mask. Moiré patterns of the two marks that are misaligned by (c) $p_{average}/4$; (d) $p_{average}/16$; (e) $p_{average}/8$; (f) 0 or integer times of $p_{average}/2$.

It can be deduced from Eq. (17) that the disparity between two sets of moirés fringes on the pattern is integer times m of period of moiré fringes only when it satisfies the condition $\Delta x = [2p_1p_2 / (p_1 + p_2)] \cdot m / 2$, where $p_{average} = 2p_1p_2 / (p_1 + p_2)$ is the weighted average of periods of two gratings, $m=0, 1, 2, \dots$

Namely, two sets of moiré fringes on the pattern become aligned only if the relative displacement of two grating marks placed on the wafer and mask is half integer times of the averaged period of two gratings. Figures 8(c) - 8(e) illustrate moiré patterns generated by

these two gratings marks that are misaligned by $p_{average}/4$, $p_{average}/8$ and $p_{average}/16$ respectively. Whereas the pattern in Fig. 8(f) corresponds to two superposed marks that are aligned or misaligned by $p_{average}m/2$.

5. Summary

On the basis of application of moiré fringes in mask alignment of photolithography, the complex amplitude distribution of moiré fringes generated from superposed gratings is analyzed in the view of Fourier optics. Two conclusions are drawn to simply summarize the rule of layout of the moiré fringes produced in the superposition of two 1D-gratings or quasi-period structures. Our analyses demonstrate that the fringes generated in the superposition of the two extended gratings can be considered as a 1D distributed moiré pattern transformed by a compound transformation which is relative to the layout of the two gratings. Especially, the 1D distributed moiré fringes of the two 1D-gratings can be expressed by an arithmetic operation of two vectors on behalf of these two 1D-gratings. In addition, the superposition of two 1D-gratings with slightly different frequencies generate period-magnified fringes which are highly sensitive to the relative shift of the two gratings. The fringe sensitivity can meet the necessity in some fields such as alignment of nanolithography.

Acknowledgment

The authors thank the financial support from 863 Program (Grant No.2006AA03z355) and Chinese natural sciences foundation Grant 60706005 and 60776029.